Centrality dependence of p_T spectra for identified hadrons in Au+Au and Cu+Cu collisions at $\sqrt{s_{NN}}=200$ GeV*

WANG Yun-Fei(王云飞)[1] SHAO Feng-Lan(邵凤兰)[1;1)] SONG Jun(宋军)[1]
WEI De-Ming(魏德明)[1] XIE Qu-Bing(谢去病)[2]

1 (Department of Physics, Qufu Normal University, Qufu 273165, China)
2 (Department of Physics, Shandong University, Jinan 250100, China)

Abstract The centrality dependence of transverse momentum spectra for identified hadrons at midrapidity in Au+Au collisions at $\sqrt{s_{NN}}$ = 200GeV is systematically studied in a quark combination model. The p_T spectra of $\pi^{\pm}$, $K^{\pm}$, $p(\bar{p})$ and $\Lambda(\bar{\Lambda})$ in different centrality bins and the nuclear modification factors (R_{CP}) for these hadrons are calculated. The centrality dependence of the average collective transverse velocity $\langle\beta(r)\rangle$ for the hot and dense quark matter is obtained in Au+Au collisions, and it is applied to a relative smaller Cu+Cu collision system. The centrality dependence of p_T spectra and the R_{CP} for π^0, K^0_s and Λ in Cu+Cu collisions at $\sqrt{s_{NN}}=200$ GeV are well described. The results show that $\langle\beta(r)\rangle$ is only a function of the number of participants N_{part} and it is independent of the collision system.

Key words relativistic high energy nucleus-nucleus collisions, nuclear modification factor, transverse collective flow, quark combination model

PACS 25.75.-q, 25.75.Ld, 25.75.Nq

1 Introduction

The hadronic collectivity is one of the important properties in ultra-relativistic heavy ion collisions. It provides a lot of information on the initial spatial anisotropy of the reaction zone[1—4], the degree of thermalization[5, 6] and the hadronization mechanism of the hot and dense medium produced in nucleus-nucleus collisions[7, 8]. It can also help to understand the broadening of jetlike particle correlations[9] and high p_T jet-quenching[10, 11]. Strong partonic multiple scatterings in nucleus-nucleus collisions would generate the collectivity of quarks, which then result in the observed collectivity of final hadrons. The quark number scaling of the hadronic elliptic flow v_2 is a piece of evidence for this original quark collectivity[12—14]. Being a key hadronization mechanism, quark combination picture has successfully described many features of multi-particle production in high energy heavy ion collisions, e.g. the high p/π ratio in intermediate transverse momentum region[15—17], the quark number scaling behavior of hadron elliptic flow[8, 18, 19] and its fine structure at small p_T[20], hadron longitudinal and transverse momentum distributions[7, 21—23], the yields and multiplicity ratios[24]. Therefore, one can extract the collectivity of the hot and dense quark matter from the data of hadrons through quark combination mechanism.

In general, the nucleus-nucleus collisions in different centralities will produce different sizes of the hot and dense quark matter. This would cause the transverse collective flow for the hot and dense quark matter varying with collision centralities. This variance of collective flow in quark level would be embodied in the transverse momentum spectra of final hadrons[25, 26] and particularly in their nuclear modification factors R_{CP}. The thermal and hydrodynamic models have described the centrality dependence of the transverse momentum distributions for final

Received 1 April 2008, Revised 11 June 2008
* Supported by National Natural Science Foundation of China (10775089, 10475049) and Science Fund of Qufu Normal University
1) E-mail: shaofl@mail.sdu.edu.cn

hadrons in low p_T region with a statistical hadronization method[27—32]. Using the quark recombination at intermediate p_T and parton fragmentation at high p_T, the Duke group in Ref. [8] has explained the strong suppression of hadron R_{CP} at high transverse momenta, and the baryon-meson difference of hadron R_{CP} in intermediate p_T region. In the present paper, with quark combination at all p_T, we use our quark combination model to study the hadron p_T spectra from central to peripheral collisions. We investigate the p_T spectra of identified hadrons at midrapidity in different centralities in Au+Au collisions at $\sqrt{s_{NN}} = 200$ GeV to obtain the centrality dependence of transverse collective flow for the hot and dense quark matter. Furthermore, we apply it to relative smaller Cu+Cu collision systems, calculate the transverse momentum spectra of final hadrons and nuclear modification factors R_{CP} in Cu+Cu collisions at $\sqrt{s_{NN}} = 200$ GeV, and compare them with the experimental data from STAR and PHENIX Collaborations.

In the next two sections, we briefly introduce the quark combination model and the transverse momentum spectra of quarks just before hadronization. The results and discussions are in Sect. 4. Summary is given in Sect. 5.

2 The quark combination model

Within the same quark combination mechanism, all kinds of combination-like models, such as recombination model[15, 21, 33], and coalescence model[16, 19], have their own features. Our quark combination model was first proposed for high energy e^+e^- and pp collisions[34—39]. Recently we have extended the model to ultra-relativistic heavy ion collisions[20, 22, 24, 40]. The model describes the production of initially produced ground state mesons (36-plets) and baryons (56-plets). In principle, it can also be applied to the production of excited states [36] and exotic states[24]. These hadrons through combination of constituent quarks are then allowed to decay into the final state hadrons. We take into account the decay contributions of all resonances of 56-plet baryons and 36-plet mesons, and cover all available decay channels by using the decay program of PYTHIA 6.1[41]. The main idea is to line up quarks and anti-quarks in a one-dimensional order in phase space, e.g. in rapidity, and let them combine into initial hadrons one by one following a combination rule. See the second section of Ref. [24] for the short description of such a rule. Of course, we also take into account the near correlation in transverse momentum by limiting the maximum transverse momentum difference for quarks and antiquarks as they combine into hadrons. The flavor $SU(3)$ symmetry with strangeness suppression in the yields of initially produced hadrons is fulfilled in the model[34, 36].

3 p_T spectra of the constituent quarks at hadronization

It is known that the measured hadron p_T spectra in relativistic heavy ion collisions exhibit a two-component behavior. The spectra take an exponential form at low p_T and a power-law form at high p_T. Based on parton-hadron duality, the transverse momentum spectra of constituent quarks just before hadronization should also have the same property. In principle, the quarks just before hadronization come from two parts, i.e. the thermal quarks from the hot medium produced in collisions and the minijet quarks from initial hard collisions. The final hadrons are the total contribution of the two parts. But, just as shown in the second figure in Ref. [8], the minijet quarks dominate the large transverse momenta where thermal quarks take a very small proportion, and thermal quarks dominate the low transverse momentum region where the minijet quarks have a small contribution. Therefore, we can neglect the two small contributions, similar to the treatment in Ref. [16], and adopt a piecewise function to describe approximately the transverse momentum distribution of constituent quarks:

$$\frac{dN_q}{2\pi p_T dp_T} = \theta(p_0-p_T)N_{th}f_{th}(p_T)+ \theta(p_T-p_0)N_{jet}f_{jet}(p_T), \qquad (1)$$

where $\theta(x)$ is the step function, N_{th} is the number of thermal quarks and N_{jet} is the number of minijet quarks. p_0 is the transition point from thermal distribution to power-law distribution, which is determined by the spectra continuity. In fact, the interaction between the thermal quarks and the minijet quarks leads to a smooth spectrum around p_0, and we neglect this effect in this paper.

The hot and dense quark matter produced in nucleus-nucleus collisions at RHIC energies shows a significant collective character[12, 13, 42]. The p_T spectra of thermal quarks at hadronization can be described by a thermal phenomenological model incorporating the transverse flow of thermal medium[43]. The quarks and antiquarks transversely boost with a flow velocity profile $\beta_r(r)$ as a function of transverse radial position r. $\beta_r(r)$ is parameterized by the surface velocity β_s: $\beta_r(r) = \beta_s\xi^n$, where $\xi = r/R_{max}$, and R_{max} is the thermal source maximum radius $(0<\xi<1)$. The transverse flow of thermal medium can be equivalently described by a superposition of a set of thermal sources, each boosted with transverse rapidity $\rho=\tanh^{-1}\beta_{\rm r}$[43]:

$$f_{\rm th}(p_{\rm T}) = \frac{{\rm d}n_{\rm th}}{2\pi p_{\rm T}{\rm d}p_{\rm T}} = A\int_0^1 \xi\,{\rm d}\xi\, m_{\rm T} \times I_0\left(\frac{p_{\rm T}\sinh\rho}{T}\right)K_1\left(\frac{m_{\rm T}\cosh\rho}{T}\right), \quad (2)$$

where A is the normalization constant in the region $p_{\rm T}\in[0,p_0]$. I_0 and K_1 are the modified Bessel functions. $m_{\rm T}=\sqrt{p_{\rm T}^2+m^2}$ is the transverse mass of the constituent quark. T is the hadronization temperature. The average transverse velocity can be written as

$$\langle\beta_{\rm r}\rangle = \frac{\int \beta_{\rm s}\,\xi^n\xi\,{\rm d}\xi}{\int \xi\,{\rm d}\xi} = \frac{2}{n+2}\beta_{\rm s}. \quad (3)$$

With fixed hadronization temperature $T=170$ MeV and parameter $n=0.5$, the average transverse velocity $\langle\beta_{\rm r}\rangle$ is able to characterize the transverse collective flow of the hot and dense quark matter.

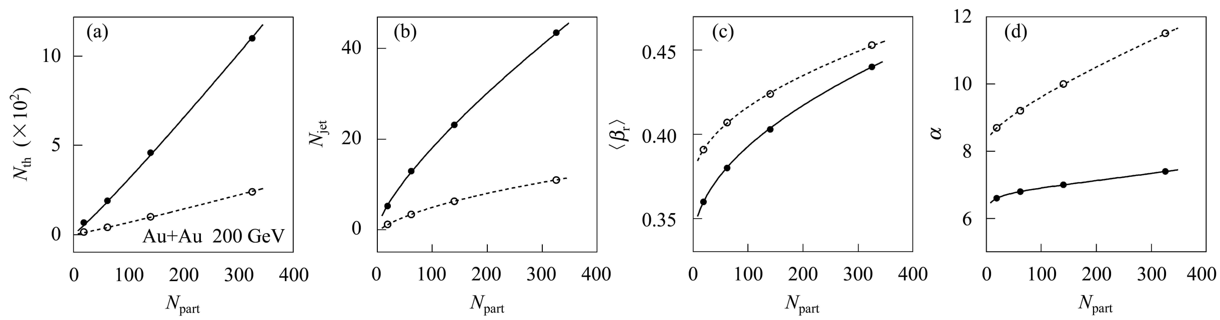

Fig. 1. The values of the parameters $N_{\rm th}$ (a), $N_{\rm jet}$ (b), $\langle\beta_{\rm r}\rangle$ (c) and α (d) for the $p_{\rm T}$ spectra of light quarks (filled circles) and strange quarks (open circles) at midrapidity in four different centrality bins. The corresponding centrality bins are 0—10%, 20%—40%, 40%—60%, and 60%—80%. The solid and dashed lines are the parameterized results for light and strange quarks respectively.

The quarks and antiquarks with high transverse momenta are mainly from the minijets created in initial hard collisions among nucleons. Here the so-called minijet quarks are those just before hadronization. They are the parton remnants after the revolution of the initial hard partons by gluon radiation and split, and are different from those in the fragmentation model. The $p_{\rm T}$ spectra of minijet quarks at hadronization can be parameterized as follows:

$$f_{\rm jet}(p_{\rm T}) = \frac{{\rm d}n_{\rm jet}}{2\pi p_{\rm T}{\rm d}p_{\rm T}} = B\left(1+\frac{p_{\rm T}}{p_0}\right)^{-\alpha}, \quad (4)$$

where B is the normalization constant in the region $p_{\rm T}\in(p_0,\infty)$.

There are four independent parameters in Eq. (1) to determine the transverse momentum distributions of quarks: $N_{\rm th}$, $N_{\rm jet}$, $\langle\beta_{\rm r}\rangle$ and α. Here, we extract the values of these parameters for the light and strange quark $p_{\rm T}$ spectra at midrapidity from the data of π^0 and $K_{\rm s}^0$[44, 45], respectively. In our quark combination model, removing the resonance decay contributions from the measured π^0 and $K_{\rm s}^0$ transverse momentum distributions, we get the initially produced π^0 and $K_{\rm s}^0$ transverse momentum spectra. The values of parameters are inversely extracted from these initial spectra. We obtain four groups of results corresponding to the centrality bins 0—10%, 20%—40%, 40%—60%, and 60%—80%. They are shown in Fig. 1. The lines in the figure are the parameterized results, from which we can get the quark $p_{\rm T}$ spectra in any collision centrality. In Fig. 2, we also show the quark $p_{\rm T}$ spectra in four collision centralities mentioned-above.

One can see from Fig. 1 that the centrality dependence of the parameter $N_{\rm th}$ is different from that of $N_{\rm jet}$. As we know, the thermal quarks which dominate the low $p_{\rm T}$ region carry most of the collision energy. The available energy used to produce hadrons in different centrality is proportional to the number of nucleon participants $N_{\rm part}$ at the fixed collision energy. Therefore, the number of thermal quarks is approximately proportional to $N_{\rm part}$. The minijet quarks with high $p_{\rm T}$ are mainly from the hard-jet created in initial hard collisions among nucleons, and their quantity is mainly determined by the number of binary collisions $N_{\rm coll}$, which is obviously different from $N_{\rm part}$. Generally, the higher the collision centrality is, the bigger the bulk volume for hot medium, the stronger the transverse collective flow β. The bigger the bulk volume for hot medium is, the more energy loss for minijet quarks, thus the steeper the minijet-quark spectra and the bigger the parameter α. It is further observed that the strange quarks are different from light quarks not only in the quantity (due to strangeness suppression) but also in the momentum distribution. It is easy to understand that the spectrum of strange quarks at high p_T, due to its heavier effective mass, is steeper than that of light quarks, i.e. $\alpha^{(s)} > \alpha^{(u,d)}$. In the low p_T range, however, the spectrum of strange quarks is flatter than the light quarks because $\beta^{(s)} > \beta^{(u,d)}$. By analyzing the data of multi-strange hadrons ϕ, Ξ and Ω, Ref. [46] also draws the same conclusion. Furthermore, the similar property is also obtained in longitudinal orientation[47]. As we know, the expansion evolution of the plasma in the partonic phase is also a process of obtaining the effective mass for partons. Due to the heavier effective mass, the strange quarks may undergo a stronger hydrodynamic expansion in the partonic phase than the light quarks.

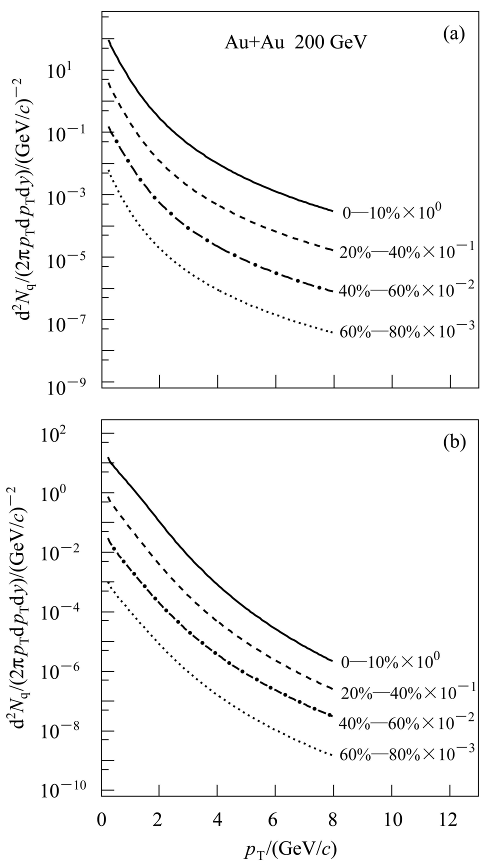

Fig. 2. The p_T spectra of the light quarks (a) and strange quarks (b) at midrapidity in Au+Au collisions at $\sqrt{s_{NN}}=200$ GeV.

As is known to all, though the nucleus-nucleus collisions at top RHIC energy exhibit a high degree of transparency, there are still a few net-quarks which stopped in the midrapidity region. The p_T spectra of both π^0 and K^0_s can not reflect the information of net quarks[40]. We obtain the number of net quarks at midrapidity in different centrality bins by fitting the rapidity densities of net-proton[26]. Note that the ratios of π^-/π^+ and $\bar{p}/p$ measured by STAR and PHENIX Collaborations reveal weak dependence of centrality and transverse momentum[26, 48]. The transverse momentum distribution of net quarks is taken to be the same as that of the newborn light quarks in the model.

With the input, we can give the transverse momentum distributions of various hadrons in different collision centralities and the nuclear modification factors R_{CP} for these hadrons. Just as mentioned in the above section, we consider the decay contributions from all available decay channels of all resonances by using the decay program of PYTHIA 6.1[41]. Therefore, we can directly compare our calculated results with the experimental data.

4 Results and discussions

4.1 The p_T spectra of hadrons in Au+Au collisions

We firstly calculate the transverse momentum spectra of $\pi^\pm$ and $p\,(\bar{p})$ in different centrality bins in Au+Au collisions at $\sqrt{s_{NN}}=200$ GeV. The results are shown in Fig. 3. Here, the pion spectra are corrected to remove the feed-down contributions from K^0_s and $\Lambda(\bar{\Lambda})$. The p_T spectra of hadrons in low p_T region are specially shown in the inserted plots. One can see that the calculated results agree well with the data from the STAR Collaboration. The strange hadron production can better reflect the property of the hot and dense quark matter produced in collisions. We also compute the transverse momentum distributions of strange hadrons $K^\pm$, $\Lambda(\bar{\Lambda})$ in different centrality bins. The results are shown in Fig. 4 and compared with the data.

As shown above, the good agreement between the model predictions and the experimental data confirms the validity of our model from the central to the peripheral collisions.

4.2 The nuclear modification factors R_{CP} for hadrons in Au+Au collisions

The nuclear modification factors R_{CP} can reflect more precisely the variation of hadron p_T spectra in different centrality bins. It is quantified as[48]:

$$R_{CP}(p_T) = \frac{\left[(d^2N/(2\pi p_T dp_T dy))/N_{bin}\right]^{Central}}{\left[(d^2N/(2\pi p_T dp_T dy))/N_{bin}\right]^{Peripheral}} \; . \tag{5}$$

In Fig. 5, we give the computed results of R_{CP} for $\pi^+ + \pi^-$ and $p+\bar{p}$ (0—10%/60%—80%), $K^\pm$ and $\Lambda+\bar{\Lambda}$ (0—5%/60%—80%), and compare them with the experimental data.

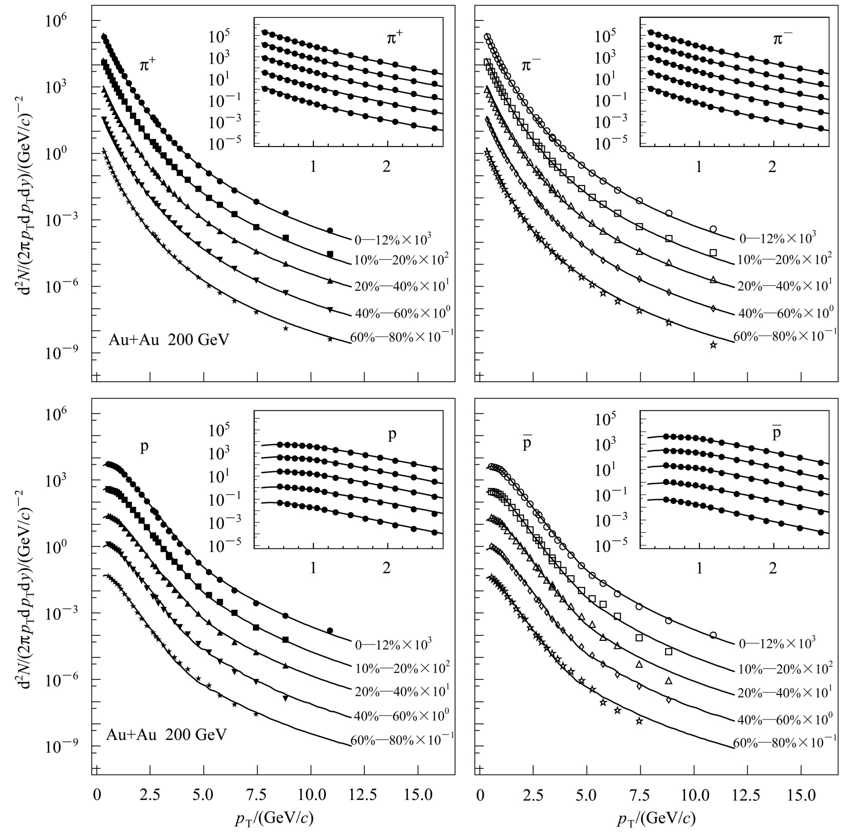

Fig. 3. The transverse momentum spectra of $\pi^{\pm}$ and $p\,(\bar{p})$ at midrapidity in different centrality bins in Au+Au collisions at $\sqrt{s_{NN}} = 200$ GeV. The data are taken from STAR Collaboration[48].

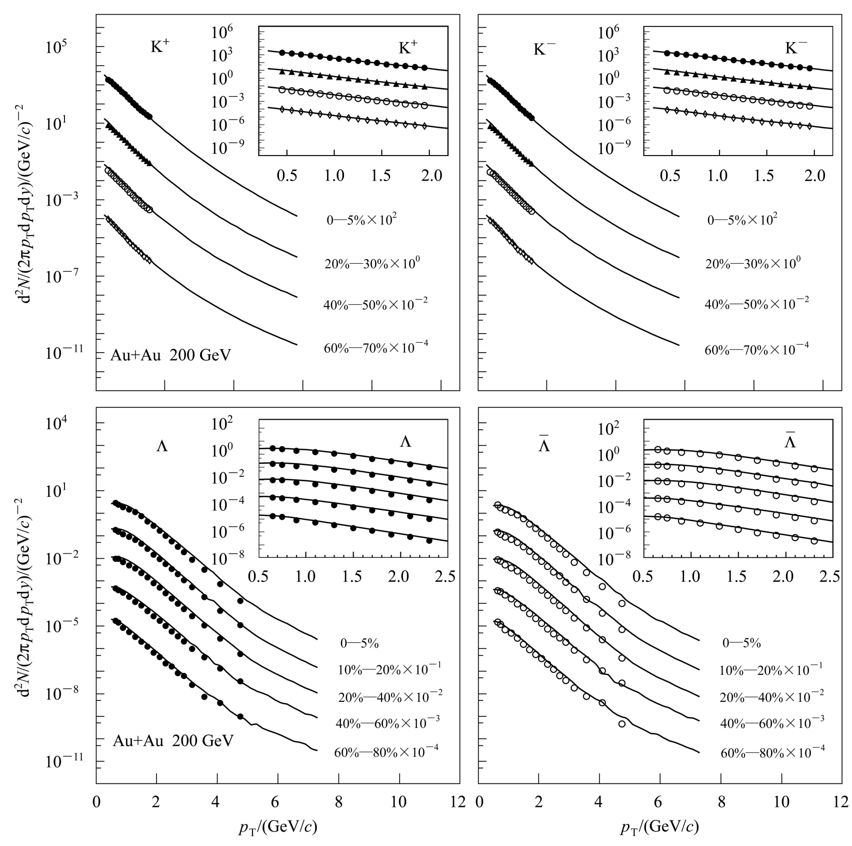

Fig. 4. The transverse momentum spectra of strange hadrons in different centrality bins in Au+Au collisions at $\sqrt{s_{NN}} = 200$ GeV. The data are taken from PHENIX and STAR Collaborations[26, 49].

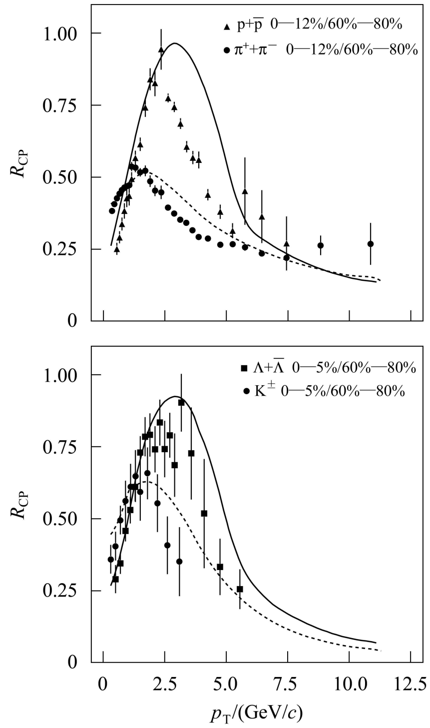

Fig. 5. The nuclear modification factors R_{CP} for identified hadrons in Au+Au collisions at $\sqrt{s_{NN}}=200$ GeV. The data are taken from STAR Collaboration[48—50].

The hadrons in low p_T region are mainly from the thermal quark combination. As shown in the first figure, the transverse collective flow of the hot and dense quark matter, denoted by $\langle\beta_r\rangle$, decreases with the falling centrality. This leads to the p_T spectra of thermal quarks becoming softer in peripheral collisions, and then results in an increasing trend of R_{CP} for hadrons in low p_T region. The hadrons with intermediate p_T are mainly produced by the combination of thermal quarks with minijet quarks. As we all know, with the decreasing collision centrality, the volume size of the hot and dense quark matter becomes small and the energy loss of minijet quarks correspondingly becomes small as they traverse the hot and dense medium. It leads to the p_T spectra of minijet quarks becoming harder in peripheral collisions, which is embodied in the decreasing value of parameter α shown in the first figure with the falling centrality. With the increasing of p_T, the hadron R_{CP} goes over from the rise caused by the combination of thermal quarks to fall caused by the combination of minijet quarks. One can see that the quark combination model well describes the behavior of R_{CP} for final hadrons in the whole p_T region considering the variation of the transverse collective flow of the hot and dense quark matter.

In addition, the data show that the R_{CP} for baryons clearly exhibits less suppression compared with that of mesons in intermediate transverse momentum region. This type dependence of R_{CP}, which is dependent upon the number of constituent quarks rather than hadronic mass, has been qualitatively discussed earlier in Refs. [8, 50] as an experimental support of the quark combination picture. Our results further manifest this baryon-meson difference of R_{CP} in intermediate p_T region.

The experimental data show that the baryon-meson difference of R_{CP} disappears at higher p_T. Using the fragmentation mechanism, the Duke group in Ref. [8] has explained this common degree of suppression for both baryons and mesons at high p_T. Our results from the quark combination can also describe this behavior of R_{CP} at high p_T. These two different hadronization mechanisms produce similar results. It suggests that the disappearance of baryon-meson difference of R_{CP} at high p_T is not caused by hadronization mechanism. The hard scatterings which take place near the surface of the collisions produce the back-to-back dijets. One-side jets escape almost without energy loss, while the away-side jets lose significant energy as they traverse the hot and dense matter. The hadrons with high p_T in all collision centralities are mostly from these jets without energy loss. The transverse momentum distributions of these minijet quarks with high p_T in central collisions, except the quantity, are almost the same with those in peripheral collisions. Therefore, no matter what the hadronization mechanism is, there exists a similar suppression of the R_{CP} for baryons and mesons at high p_T.

It is also observed that the calculated R_{CP} deviates from the data to a certain degree. The reason may be that some effects, such as the production of excited-state hadrons and final-state rescattering, are not considered currently in the model. As we know, a small quantity of the excited-state hadrons are produced in relativistic heavy ion collisions, and the yields and momentum distributions of final hadrons are influenced by the decay contribution of these excited-state hadrons to a certain extent. As the decay branch ratios of many excited-state hadrons are incompletely measured, the contributions of excited-state hadrons are neglected in the current model. On the other hand, the perfect quark-number scaling of hadron elliptic flow v_2 suggests that the influence of final-state rescattering on hadron distribution is finite and small[12], so we also neglect it in the work. These two effects would affect the fine observable R_{CP}.

4.3 The p_T spectra and nuclear modification factors R_{CP} for hadrons in Cu+Cu collisions

Now, we apply the centrality (participants) dependence of parameters in Au+Au collisions which

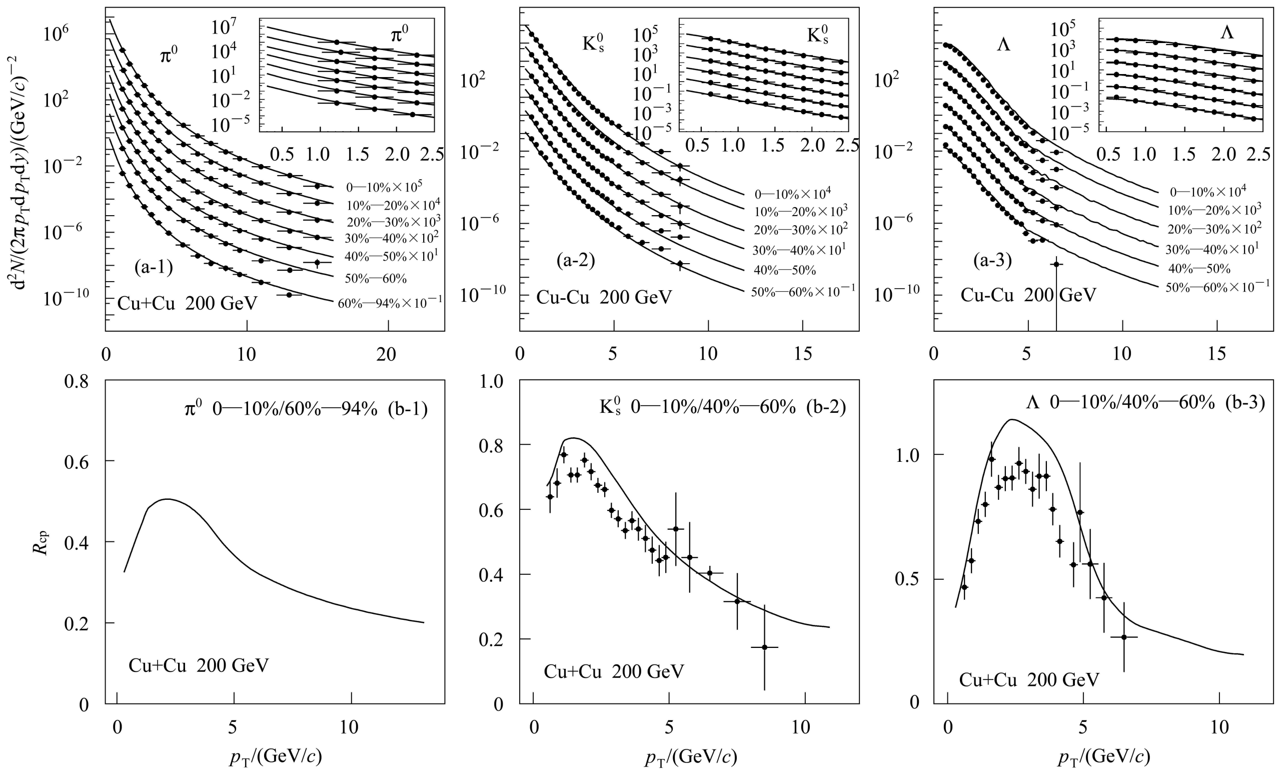

Fig. 6. The transverse momentum spectra of identified hadrons in different centrality bins (a) and their nuclear modification factors $R_{\rm CP}$ (b) in Cu+Cu collisions at $\sqrt{s_{\rm NN}}=200$ GeV. The data are taken from PHENIX and STAR Collaborations[44, 51].

determine the $p_{\rm T}$ spectra of quarks in different centralities, to the relative smaller Cu+Cu collision system at $\sqrt{s_{\rm NN}}=200$ GeV. In Fig. 6, we show the calculation results for the transverse momentum spectra of π^0,$\rm K^0_s$ and hyperon Λ in different centrality bins and $R_{\rm CP}$ for these hadrons in Cu+Cu collisions at $\sqrt{s_{\rm NN}}=200$ GeV. The $p_{\rm T}$ spectra of hadrons in low $p_{\rm T}$ region are specially shown in the inserted plots. We find that the results agree well with the data in the low transverse momentum region in all centrality bins. This implies that the transverse collective flow of the hot and dense quark matter, i.e. $\langle\beta_{\rm r}\rangle$, is only a function of $N_{\rm part}$ and irrelevant to the collision system at the same collision energy. The good agreement of our results with the π^0 data at high transverse momenta also suggests that the energy loss of mini-jet quarks in Cu+Cu collisions is almost the same with that in Au+Au collisions with the same participants $N_{\rm part}$ at $\sqrt{s_{\rm NN}}=200$ GeV. It is consistent with the recent measurement of STAR Collaboration[52, 53]. The above results suggest that the hot and dense quark matter produced in Au+Au and Cu+Cu collisions at the same $N_{\rm part}$ and collision energy has similar strong-interacting character. Of course, even at the same $N_{\rm part}$ and collision energy, the initial spatial eccentricity of the overlap collision geometry in Au+Au collisions is obviously different from that in Cu+Cu collision systems. The difference is clearly reflected by some important observations, e.g. the elliptic flow of final hadrons and the global polarization of hyperon[12, 50, 54—56].

5 Summary

Using the quark combination model, we study systematically the centrality dependence of the transverse momentum distributions for the identified hadrons at midrapidity in Au+Au and Cu+Cu collisions at $\sqrt{s_{\rm NN}}=200$ GeV. The centrality dependence of the parameters for quark $p_{\rm T}$ spectra is extracted from the data of π^0 and $\rm K^0_s$ in Au+Au collisions. We calculate the transverse momentum distributions of $\pi^{\pm}$, $\rm p\,(\bar{p})$, $\rm K^{\pm}$ and $\Lambda(\bar{\Lambda})$ in five centrality bins. The good agreement between our results and the data indicates that the quark combination hadronization mechanism is applicable to all collision centralities. The nuclear modification factors $R_{\rm CP}$ for $\pi^++\pi^-$ and $\rm p+\bar{p}$ (0—10%/60%—80%), $\rm K^{\pm}$ and $\Lambda+\bar{\Lambda}$ (0—5%/60%—80%) are calculated and compared with the data. The quark combination model well describes the behavior of $R_{\rm CP}$ for final hadrons in the whole $p_{\rm T}$ region considering the decrease of the transverse collective flow of the hot and dense quark matter from the central collisions to the peripheral collisions. The disappearance of the baryon-meson difference of R_{CP} at higher p_T is derived from the same transverse momentum distribution of minijet quarks between the central and the peripheral collisions rather than the hadronization mechanism. Furthermore, we apply the N_{part} dependence of parameters to the relative smaller Cu+Cu collision system at the same collision energy. We calculate the transverse momentum spectra of π^0, K_s^0, and Λ at midrapidity in different centrality bins and R_{CP} of these hadrons in Cu+Cu collisions at $\sqrt{s_{NN}}=200$ GeV. The results agree well with the data in low transverse momentum region in all centrality bins. It suggests that the transverse collective flow of the hot and dense quark matter is only the function of N_{part} and independent of collision system. The calculated π^0 spectrum at high p_T is also in good agreement with the data. These results suggest that the hot and dense quark matter produced in Au+Au and Cu+Cu collisions at the same N_{part} and collision energy has similar strong-interacting character.

We are grateful to Wang Q., Liang Z. T., Yao T. and Han W. for helpful discussions.

References

1 Reisdorf W, Ritter H G. Annu. Rev. Nucl. Part. Sci., 1997, **47**: 663—709
2 Sorge H. Phys. Rev. Lett., 1999, **82**: 2048—2051
3 Kolb P, Sollfrank J, Heinz U. Phys. Lett. B, 1999, **459**: 667—672
4 Teaney D, Shuryak E V. Phys. Rev. Lett., 1999, **83**: 4951—4954
5 Kolb P, Sollfrank J, Heinz U. Phys. Rev. C, 2000, **62**: 054909
6 Voloshin S A, Poskanzer A M. Phys. Lett. B, 2000, **474**: 27—32
7 Greco V, Ko C M, Levai P. Phys. Rev. C, 2003, **68**: 034904
8 Fries R J, Müller B, Nonaka C et al. Phys. Rev. C, 2003, **68**: 044902
9 Armesto N, Salgado C A, Wiedemann U A. Phys. Rev. Lett., 2004, **93**: 242301
10 WANG X N, Gyulassy M. Phys. Rev. Lett. C, 1992, **68**: 1480—1483
11 Armesto N, Salgado C A, Wiedemann U A. Phys. Rev. C, 2005, **72**: 064910
12 Adare A et al. (PHENIX Collaboration). Phys. Rev. Lett., 2007, **98**: 162301
13 Adare A et al. (PHENIX Collaboration). Phys. Rev. Lett., 2003, **91**: 182301
14 Enokizono A (the PHENIX Collaboration). Nucl. Phys. A, 2007, **787**: 37c—43c
15 Fries R J, Müller B, Nonaka C et al. Phys. Rev. Lett., 2003, **90**: 202303
16 Greco V, Ko C M, Levai P. Phys. Rev. Lett., 2003, **90**: 202302
17 Hwa R C, YANG C B. Phys. Rev. C, 2003, **67**: 034902
18 Voloshin S A. Nucl. Phys. A, 2003, **715**: 379c—388c
19 Molnar D, Voloshin S A. Phys. Rev. Lett., 2003, **91**: 092301
20 YAO T, XIE Q B, SHAO F L. Chin. Phys. C, 2008, **32**: 356—362
21 Hwa R C, YANG C B. Phys. Rev. C, 2004, **70**: 024905
22 SHAO F L, YAO T, XIE Q B. Phys. Rev. C, 2007, **75**: 034904
23 Hwa R C, Tian Z. Phys. Rev. C, 2005, **72**: 024908
24 SHAO F L, XIE Q B, WANG Q. Phys. Rev. C, 2005, **71**: 044903
25 Arsene I et al. (BRAHMS Collaboration). Phys. Rev. C, 2005, **72**: 014908
26 Adler S S et al. (PHENIX Collaboration). Phys. Rev. C, 2004, **69**: 034909
27 Schnedermann E, Heinz U. Phys. Rev. Lett., 1992, **69**: 2908—2911
28 Kolb P F, Rapp R. Phys. Rev. C, 2003, **67**: 044903
29 Nonaka C, Bass S A. Phys. Rev. C, 2007, **75**: 014902
30 Heinz U, Kolb P. Nucl. Phys. A, 2002, **702**: 269—280
31 Huovinen P. Nucl. Phys. A, 2005, **761**: 296—312
32 Prorok D. Phys. Rev. C, 2006, **73**: 064901
33 Pratt S, Pal S. Phys. Rev. C, 2005, **71**: 014905
34 XIE Q B, LIU X M. Phys. Rev. D, 1988, **38**: 2169—2177
35 LIANG Z T, XIE Q B. Phys. Rev. D, 1991, **43**: 751—759
36 WANG Q, XIE Q B. J. Phys. G, 1995, **21**: 897—904
37 ZHAO J Q, WANG Q, XIE Q B. Sci. Sin. A, 1995, **38**: 1474—1487
38 WANG Q, SI Z G, XIE Q B. Int. J. Mod. Phys. A, 1996, **11**: 5203—5210
39 SI Z G, XIE Q B, WANG Q. Commun. Theor. Phys., 1997, **28**: 85—94
40 SONG J, SHAO F L, XIE Q B et al. The Influence of Net-Quarks on the Yields and Rapidity Spectra of Identified Hadrons. arXiv: hep-ph/0801.0918
41 Sjostrand T, Eden P, Friberg C et al. Comput. Phys. Commun., 2001, **135**: 238—259
42 Abelev B I et al. (STAR Collaboration). Phys. Rev. Lett., 2007, **99**: 112301
43 Schnedermann E, Sollfrank J, Heinz U. Phys. Rev. C, 1993, **48**: 2462—2475
44 Sakaguchi T. (PHENIX Collaboration). Contributions for Quark Matter 2006 Poster Session. Shanghai, China, 14—20 November, 2006. arXiv: nucl-ex/0703027
45 Adams J et al. (STAR, STAR-RICH Collaborations). nucl-ex/0601042
46 CHEN J H, JIN F, Gangadharan D et al. Parton Distribution at Hadronization from Bulk Dense Matter Produced at RHIC. arXiv: 0801.2265[nucl-th]
47 SONG J, SHAO F L, XIE Q B et al. Rapidity Dependence of Hadron Production in Central Au+Au Collisions at $\sqrt{s_{NN}}=200$ GeV. arXiv: nucl-th/0703095
48 Abelev B I et al. (STAR Collaboration). Phys. Rev. Lett., 2006, **97**: 152301
49 Admas J et al. (STAR Collaboration). Phys. Rev. Lett, 2006, **98**: 062301
50 Adams J et al. (STAR Collaboration). Phys. Rev. Lett., 2003, **92**: 052302
51 Timmins A R. (STAR Collaboration). Quark Matter 2006 Proceedings. Shanghai, China, 14—20 November, 2006. arXiv: nucl-ex/0708.3290
52 Hollis R S. (STAR Collaboration). Proceedings for the Lake Louise Winter Institute 2007. Alberta, Canada, 19—24 February 2007. arXiv: nucl-ex/0705.0686
53 Bekele S. (BRAHMS Collaboration). arXiv: nucl-ex/0601011
54 LIANG Z T, WANG X N. Phys. Rev. Lett., 2005, **94**: 102301
55 Abelev B I et al. (STAR Collaboration). Phys. Rev. C, 2007, **76**: 024915
56 Back B B et al. (PHOBOS Collaboration). Phys. Rev. Lett., 2002, **89**: 222301